ACADEMIA ROMÂNĂ
Revue Roumaine de Chimie
http://web.icf.ro/rrch/

Rev. Roum. Chim.,
2018, *63*(9), 821-828

Dedicated to Niculae I. Ionescu PhD
on the occasion of his 85th anniversary

IMPACT OF $RbLaTa_2O_7$ LAYERED PEROVSKITE SYNTHESIS CONDITIONS ON THEIR ACTIVITY FOR PHOTOCATALYTIC ABATEMENT OF TRICHLOROETHYLENE

Monica RACIULETE, Florica PAPA, Daniela C. CULITA, Cornel MUNTEANU, Irina ATKINSON, Veronica BRATAN, Jeanina PANDELE-CUSU, Razvan STATE and Ioan BALINT*

"Ilie Murgulescu" Institute of Physical Chemistry of the Roumanian Academy, 202 Spl. Independenței 060021 Bucharest, Roumania

Received July 27, 2017

In this study, we report the synthesis and characterization of $RbLaTa_2O_7$ layered perovskite obtained by conventional solid-state reaction at 1100 °C at two reaction times, 10 h and 18 h. XRD results showed that prolonging the reaction time highly affected the phase composition of the obtained solids. The photocatalytic test results indicate that RbLaTa-10h sample shows better performance for abatement of trichloroethylene (TCE) compared to RbLaTa-18h, under simulated solar light irradiation. The enhanced photocatalytic activity is attributed to the larger amount of surface -OH groups which are responsible for generation of strongly oxidizing hydroxyl radicals. Significant values of TCE conversion, after 18 h of reaction time, makes the obtained layered perovskite suitable candidate for the photocatalytic abatement of harmful chlorinated compounds.

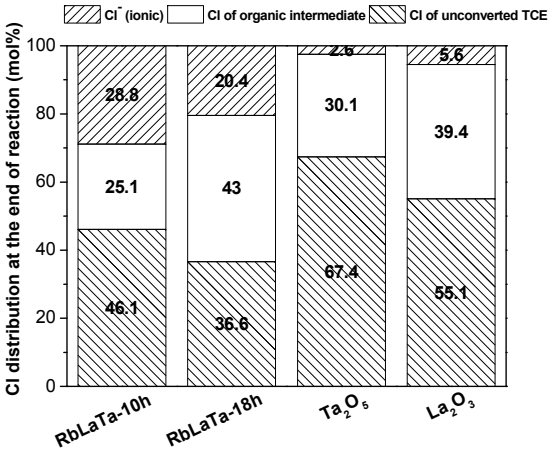

INTRODUCTION

In the world, sunlight is the most abundant and cheapest source of energy. One of the major goals of material sciences and engineering is development of efficient photocatalysts able to convert this energy into hydrogen via water splitting and for removal of harmful pollutants.

Trichloroethylene (TCE) is a halogenated volatile organic compound (Cl-VOC) widely employed as solvent in degreasing operations, as well as a chemical intermediate to produce polyvinyl chloride.[1] This contaminant frequently detected in groundwater pose significant threats to the environment and human health. The U.S. Environmental Protection Agency (EPA) stated a strict control on the maximum contaminant level (MCL) of 5 ppb for TCE in drinking water. Among various technologies applied for abatement of chlorinated contaminants, photocatalytic mineralization is a sustainable and cost-effective alternative due to its excellent selectivity towards formation of

*Corresponding author: ibalint@icf.ro

harmless products.[2] To date, titanium dioxide which is by far the most commonly studied photocatalyst, has been investigated by numerous research groups for removal of chlorinated organic pollutants.[3,4] Recent studies performed by State *et al*.[5] revealed that TCE is converted efficiently (> 80 %) to final reaction products (namely Cl^- and CO_2) over Au/TiO_2 and $PdAu/TiO_2$ by combined photomineralization/hydrodechlorination processes under simulated solar light (SSL). Other types of materials such as nano-ZnO/Laponite composite[6] have been successfully applied as photocatalysts for remediation of polluted waters.

Alkali tantalate photocatalysts have received significant attention due to their optical and electronic properties.[7,8] Tantalate perovskites with layered structure are excellent photocatalysts not only for splitting of water but also for the degradation of environmental pollutants. Their general formula is $A[A'_{n-1}B_nO_{3n+1}]$ where A is an alkali metal, A' is a lanthanide, B is a d_0 transitional metal and *n* represents the number of perovskite layers. $RbNdTa_2O_7$ photocatalyst had been reported to display the highest efficiency for decomposition of water into stoichiometric H_2 and O_2 among the $RbLnTa_2O_7$ (La, Pr, Nd and Sm) catalysts investigated by Machida's group.[9] $Sr_2Ta_2O_7$ and $Sr_2Nb_2O_7$ with similar layered perovskite structure showed activities for the same reaction without any additives under UV light.

The present study deals with the impact of $RbLaTa_2O_7$ layered perovskite synthesis conditions on their activity for the photocatalytic abatement of trichloroethylene under simulated solar irradiation.

EXPERIMENTAL

RbLaTa-based layered perovskites synthesis

$RbLaTa_2O_7$ layered perovskite was synthesized by solid-state reaction using tantalum pentoxide (Ta_2O_5, ≥ 99%, Alfa Aesar), lanthanum oxide (La_2O_3, ≥ 99%, Sigma-Aldrich), and rubidium carbonate (Rb_2CO_3 ≥ 98 %, Fluka AG) as precursors. The Rb/La/Ta molar ratio was 1/1/2. The precursor powders were homogeneously mixed and calcined in air atmosphere at 1100 °C for 10 and 18 h, respectively. A 50% molar excess of the alkali source was used to compensate the loss by volatilization of Rb cations during heating. The resultant solids were thoroughly washed with distilled water and dried at 110 °C in air. The two samples were hereafter labeled as RbLaTa-10h and RbLaTa-18h, depending on the calcination time.

Samples characterization

The crystalline phases of samples were identified by using a powder X-ray diffractometer (Rigaku Ultima IV) with monochromatic Cu Kα radiation (λ = 1.5418 Å). The crystallite size was calculated employing Debye-Scherrer equation. Thermo-differential analyses (TG/DTA) were recorded with Mettler Toledo TGA/SDTA 851[e] apparatus in air atmosphere using an alumina crucible. The temperature range was set between 25 – 1400 °C at a heating rate of 10 °C·min^{-1}. The morphology of the powders was observed by scanning electron microscopy (SEM) using FEI Quanta3D FEG instrument at an accelerating voltage of 5 kV, in high-vacuum mode with Everhart–Thornley secondary electron (SE) detector coupled with EDX analysis. Specific surface areas were determined by N_2 physisorption at 77 K using a Micrometrics ASAP 2020 apparatus. Prior to analysis, samples were outgassed under vacuum at 200 °C for 12 h. UV-Vis spectra were recorded with a Perkin Elmer Lambda 35 spectrophotometer equipped with integrating sphere. The reflectance was converted to absorption using Kubelka-Munk function. The optical band gap of the samples was calculated from the absorption spectra, using the equation E(eV) =1240.8/λ (nm). IR spectra were obtained with a JASCO 4100 spectrophotometer in the range 400 – 4000 cm^{-1} using the KBr pellet technique.

Photocatalytic abatement of TCE under simulated solar irradiation

The photocatalytic abatement of trichloroethylene (TCE) was conducted under simulated solar light using a 150 W short-arc Xe lamp (1000 Wm^2, Peccel-L01) at 18 °C. A powder sample of the perovskite (0.05 g) was suspended in distilled water (110 mL) by use of a magnetic stirring bar. An appropriate amount of TCE solution was injected into the photoreactor to obtain a final concentration of 50 mg·L^{-1}). The system was allowed to stay in dark for 80 min, under stirring, to attain the adsorption equilibrium. The concentration TCE was determined by head space analysis at 30 min time interval by gas chromatography [Agilent 7890A, equipped with a flame ionization detector (FID) and an HP-PlotQ capillary column (30m × 0.53 mm)]. The concentration of chloride ions (Cl^-) was determined by ion chromatography (Dionex ICS 900).

RESULTS AND DISCUSSION

Crystal structure of the synthesized $RbLaTa_2O_7$ layered perovskites

The influence of thermal treatment on final crystalline structure and on the morphology of the as-synthesized $RbLaTa_2O_7$ layered perovskites was assessed by changing the calcination time from 10 h to 18 hours. Only a small amount of $RbLaTa_2O_7$ layered perovskite phase (PDF card no. 01-089-0389) was formed during calcination at 1100 °C for 10 h (Fig.1 and Table 1). The appearance of La_3TaO_7 transient phase (PDF card no. 01-073-8085) and some weak diffraction lines ascribable to unreacted La_2O_3 (PDF card no. 00-005-0602) can be also identified in diffractogram. Extending the thermal treatment time from 10 h to 18h at the same temperature, *i.e.* RbLaTa-18h

sample, formation of $RbLaTa_2O_7$ as major phase take place along with appearance of supplementary diffraction lines assigned to $LaTa_3O_9$ (PDF card no. 01-079-1294), $LaTaO_4$ (PDF card no. 01-072-7771) and $RbLaO_2$ (PDF card no. 00-030-1069). Two diffraction lines situated at 2θ of 6.86° for RbLaTa-10h and 6.32° for RbLaTa-18h could not be ascribed with certitude to an indexed crystalline phase. It can be seen that for longer thermal treatment time, the crystallinity of the products was improved and the amount of the $RbLaTa_2O_7$ target phase increased. The average crystallite sizes calculated from the (102) diffraction line of $RbLaTa_2O_7$ phase (2θ = 28.2 °) using the Debye-Scherrer equation were 14.1 nm for RbLaTa-10h solid and 11.0 nm in the case of the solid treated at 1100 °C for 18 h (*i.e.* RbLaTa-18h). The specific surface area of RbLaTa-10h sample is half compared to RbLaTa-18h solid (4 and 8 m^2g^{-1}, respectively, Table 1). The surface area results correlate well with XRD outcome (Table 1) as higher surface area corresponds to smaller crystallite size.

Thermal analyses were performed to evidence the solid-state reactions taking place between precursors during the synthesis. Fig. 2 depicts the curves for Rb_2CO_3 – La_2O_3 – Ta_2O_5 mixtures recorded from room temperature to 1400 °C.

Table 1

Preparation conditions, phase composition, particle size and specific surface areas of the synthesized samples. The stoichiometric ratio of Rb/La/Ta was 1/1/2

Sample name	Reaction temperature (°C)	Reaction time (h)	Phase composition	Crystallite size, from XRD (nm)*	S_{BET} ($m^2 \cdot g^{-1}$)
RbLaTa-10h	1100	10	$RbLaTa_2O_7$, La_3TaO_7, La_2O_3, unidentified phase	14.1	4
RbLaTa-18h	1100	18	$RbLaTa_2O_7$, $LaTa_3O_9$, $LaTaO_4$, $RbLaO_2$, unidentified phase	11.0	8

*Crystallite size calculated for (102) reflexion of $RbLaTa_2O_7$ tetragonal layered perovskite phase, using Debye-Scherrer equation.

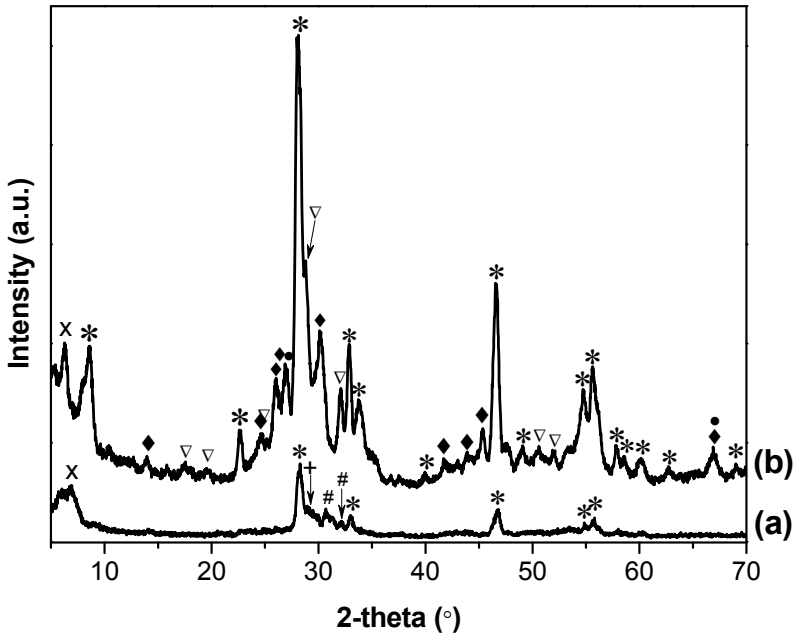

Fig. 1 – XRD patterns of the perovskite samples treated at 1100 °C for (a) 10 h and (b) 18 h.
(✱ - $RbLaTa_2O_7$, # - La_3TaO_7, ▽ - $LaTaO_4$, ✚ - La_2O_3, ♦ - $LaTa_3O_9$, ●- $RbLaO_2$, x- unidentified phases).

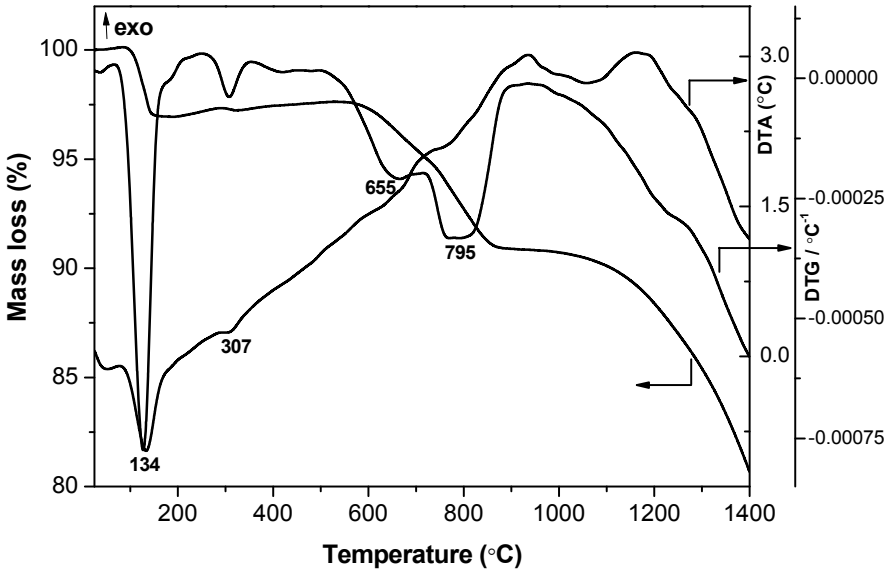

Fig. 2 – TG – DTG - DTA curves recorded to evidence the solid state reactions between Rb_2CO_3, La_2O_3 and Ta_2O_5 precursors from room temperature to 1400 °C with a heating rate of 10 °C min^{-1}.

DTA curve shows two endothermic peaks between room temperature and 500 °C. The first one centered at 134 °C accompanied by a mass loss of 3% corresponds to the elimination of adsorbed water and the second one with maximum peak at 309 °C which can be due to a partial dehydration of La_2O_3 owing to its sensitivity to atmosphere.[10] In the temperature range of 500 - 880 °C, a two-step mass loss is observed. The first one (maximum DTG peak at 655 °C) with a weight loss of 2.4 % assigned to removable adsorbed CO_2 species from La_2O_3 and the second stage of 4.2 % is attributed to the elimination of CO_2 from rubidium carbonate. Even if the XRD analysis really does not show the presence of any carbonate phases and La_2O_3 was pre-heated before reaction, thermal analysis reveals that carbonation of lanthanum oxide can occur according to the electronegativity of elements (Rb = 0.98; La = 1.30 and Ta = 1.92).[11] After 880 °C, the TG curve displays a slight mass loss which became more accentuated at temperatures higher than 1100 °C. This fact is in agreement with literature data[12] suggesting that the formation of $RbLaTa_2O_7$ phase is accompanied by a significant weight loss. Also, at this stage multiple reactions take place with the formation of intermediate phases such as La_3TaO_7, $LaTa_3O_9$, $LaTaO_4$, or $RbLaO_2$. It is well known that the binary phase diagram of La_2O_3 – Ta_2O_5 includes four components: La_3TaO_7, $LaTaO_4$, $LaTa_3O_9$ and $La_2Ta_{12}O_{33}$.[13] The XRD pattern of our solid synthesized at 1100 °C confirms the formation of La_3TaO_7, $LaTaO_4$, and $LaTa_3O_9$ intermediate products which finally leads to $RbLaTa_2O_7$ layered perovskite phase.

Microstructure and optical properties of RbLaTa-based photocatalysts

In order to understand the morphological evolution of the synthesized solids a thermal treatment SEM analysis was carried out. Fig. 3 highlights that reaction time is a key parameter, determining the morphology (shape and particle size) of layered perovskites.

Well-developed $RbLaTa_2O_7$ nanowires homo-centrically grown which tend to form bundles along with a small amount of agglomerated nanoparticles can be observed in the case of RbLaTa-10h layered perovskite (Figs. 3a and 3b). The width of nanowires is in the range of 40 -80 nm and the bundles can reach up to 300 nm in diameter. With the reaction time extended to 18 h, the nanoparticles disappeared and a tendency of the nanowires to split on occurs (Figs. 3c and 3d).

IR spectra of the RbLaTa-10h and RbLaTa-18h perovskite samples prepared at 1100 °C (Fig. 4) shows several absorption bands at lower wavenumbers (bands at 464, 620 and 883 cm^{-1}) characteristic to Rb–O, M – O (M = Ta or La), and M–O–M stretching vibrational modes. The band at 1396 cm^{-1} is assigned to the unidentate carbonate species while the band located at 1646 cm^{-1} corresponds to H-O-H bending mode of water molecules adsorbed on the surface of the

perovskite. The broad bands observed in the high-wavenumbers region (2500 – 3700 cm^{-1}) with a shoulder at 3232 cm^{-1} corresponds to the stretching vibration of O-H groups.[14] From 3232 cm^{-1} peak amplitude it can be stated that the concentration of surface -OH groups on RbLaTa-10h is considerable higher compared to RbLaTa-18h sample. This implies that synthesis carried out at longer reaction time lowers the density of surface hydroxyl groups, which are considered to be the main source of hydroxyl radicals (•OH) responsible for the photomineralization of TCE.

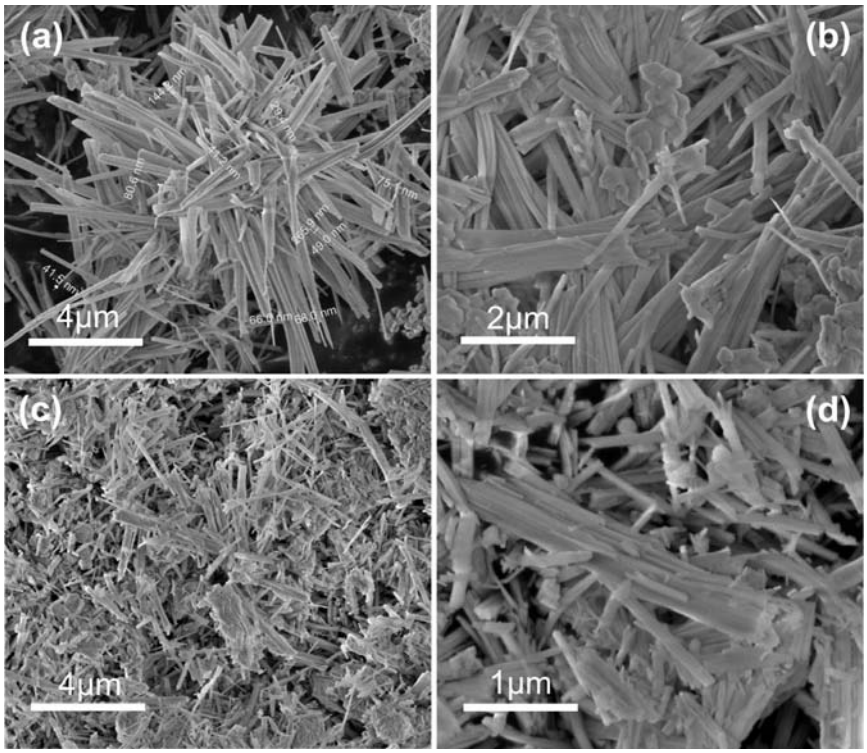

Fig. 3 – SEM images of $RbLaTa_2O_7$ layered perovskite samples treated at 1100 °C after reaction times of (a-b) 10 h and (c-d) 18 h, respectively.

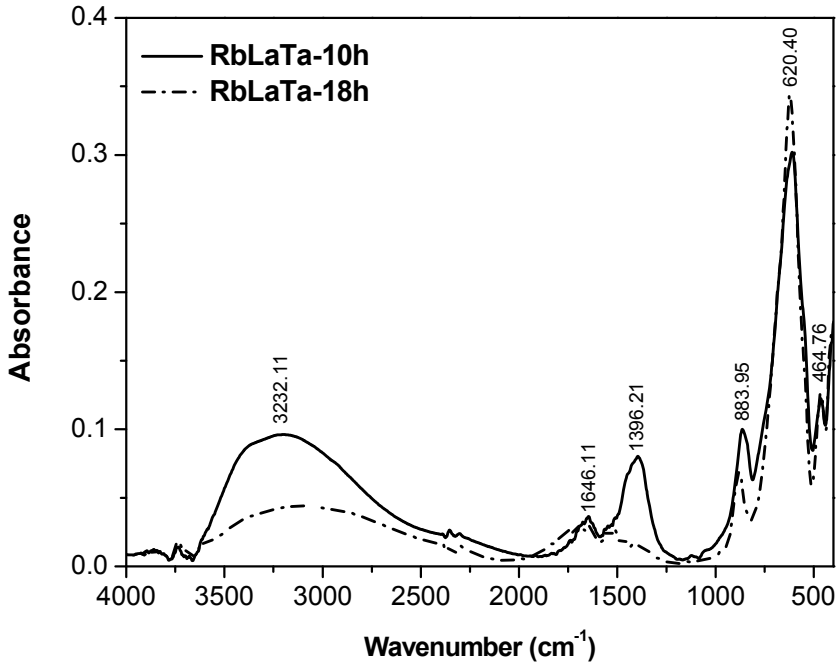

Fig. 4 – FTIR spectra of RbLaTa-10h and RbLaTa-18 h photocatalysts.

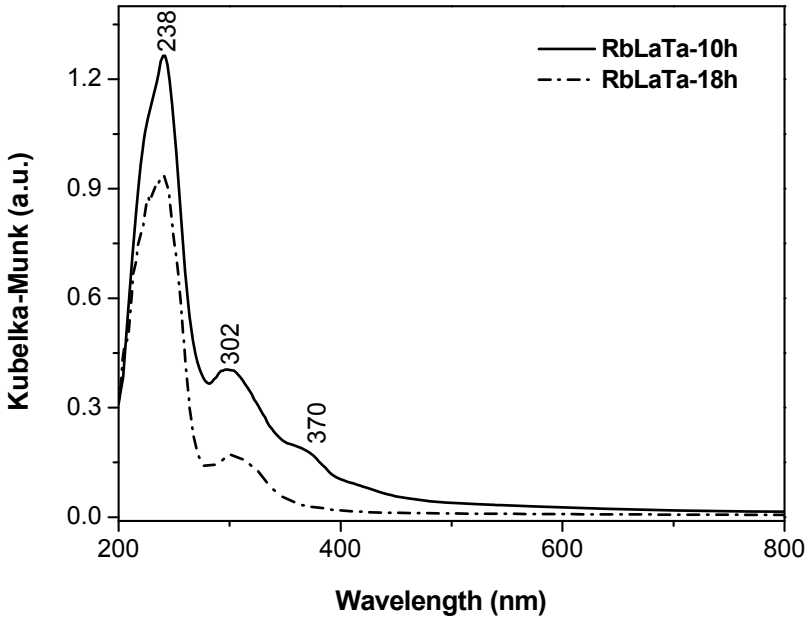

Fig. 5 – UV-Vis absorption spectra of the RbLaTa-10h and RbLaTa-18h photocatalysts.

The UV-Vis absorption spectra of $RbLaTa_2O_7$ layered perovskites synthesized at 1100 °C and two annealing times (Fig. 5) show similar absorption bands with maximum located at 238 and 302 nm (for both samples), together with another band at 370 nm (only shown for RbLaTa-10h). These absorption bands correspond to excitation from the O 2p valence band to the Ta 5d conduction band. For RbLaTa-10h sample, the absorption onset occurs at 392 nm corresponding to band gap energy of 3.1 eV, while in the case of RbLaTa-18h solid the absorption edge occurs at 363 nm obtaining a band gap of 3.4 eV. The band gap values of the prepared RbLaTa-10h and RbLaTa-18h samples were lower than those reported in previous studies by Machida and coll.[9] (Eg of $RbLaTa_2O_7$ was 3.9 eV) but are closer to the Eg value found by Maggard and co-workers of 3.3 eV for the same phase.[15]

Photocatalytic abatement of TCE over $RbLaTa_2O_7$ layered perovskite catalysts

Trichloroethylene (TCE), employed to evaluate the photocatalytic performances of the $RbLaTa_2O_7$ layered perovskites, was selected as a model chlorinated volatile organic compound (Cl-VOC) because it is a widespread groundwater pollutant. Cl^- anion and carbon dioxide are the desirable final reaction products of the complete mineralization of TCE. For comparison, the photocatalytic results of Ta_2O_5 and La_2O_3 references were also performed.

The evolution of TCE concentration over as-synthesized $RbLaTa_2O_7$ layered perovskites and the parental references after 5 h of irradiation time is presented in Fig. 6A. Both photocatalysts exhibit resembling activity of 0.20 $mmol \cdot L^{-1}$ and 0.18 $mmol \cdot L^{-1}$ over RbLaTa-10h and RbLaTa-18h catalysts, respectively. The activities of Ta_2O_5 and La_2O_3 references were lower than that of RbLaTa-based layered perovskites (the decrease in TCE concentration of references was 0.32 $mmol \cdot L^{-1}$ and 0.26 $mmol \cdot L^{-1}$, respectively).

Fig. 6B presents the amount of Cl^- (expressed in $mmol \cdot L^{-1}$) released during the photodegradation of TCE in time over the RbLaTa-10h and RbLaTa-18h photocatalysts and compared to references. Both samples show an increased Cl^- release rate in the first hour of irradiation. The reaction rate of Cl^- formation after 1 hour of irradiation time (expressed in $mmol \cdot h^{-1}$) increases as follows: RbLaTa-10h ($5.50 \cdot 10^{-3}$) > RbLaTa-18h ($3.16 \cdot 10^{-3}$) > La_2O_3 ($0.51 \cdot 10^{-3}$) > Ta_2O_5 ($0.25 \cdot 10^{-3}$). Then the Cl^- formation rate is stabilized to a constant value. The order of activity follows the sequence: RbLaTa-10h > RbLaTa-18h > La_2O_3 > Ta_2O_5.

Fig. 7 represents the conversion of TCE *versus* the time after 5 hours of irradiation over the as-synthesized layered perovskites and references. Results indicate that the conversion values on Ta_2O_5 and La_2O_3 are the lowest (33 % and 45 % respectively), followed by RbLaTa-10h solid with 59%. The highest conversion value (63 %) is reached over the perovskite synthesized at 1100 °C for 18 h, *i.e.* RbLaTa-18h. The TCE conversion results suggest that increased surface area favors the adsorption of pollutant on the catalyst, improving TCE transformation either in intermediates or in final mineralization products.[16]

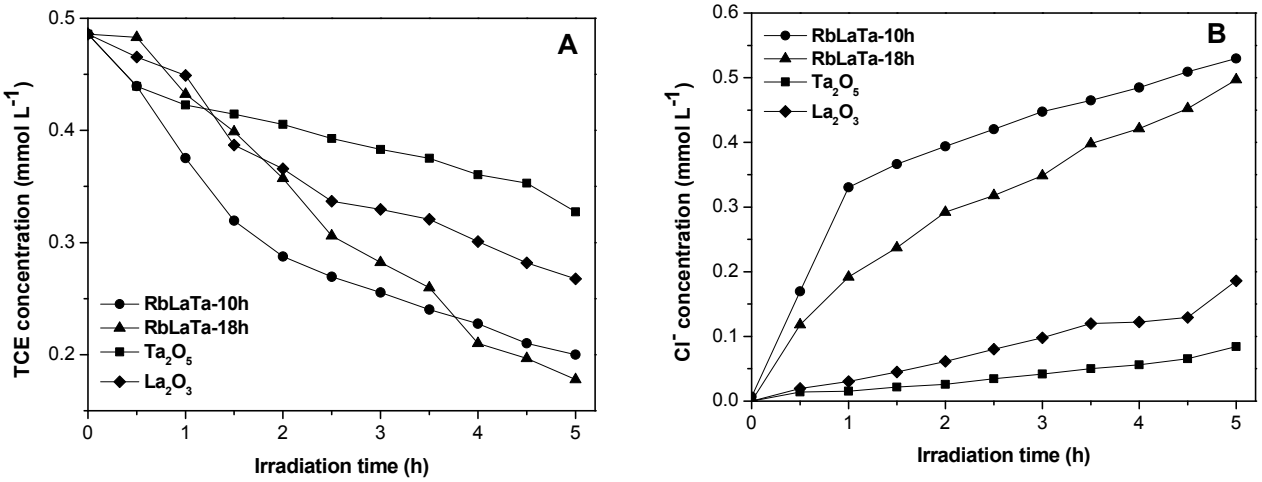

Fig. 6 – Time-evolution of (A) TCE and (B) Cl^- concentrations over RbLaTa-10h and RbLaTa-18h photocatalysts and the reference compounds. Reaction conditions: initial concentration of TCE = 5 $mg \cdot L^{-1}$; simulated solar irradiation, T = 18 °C, $m_{catalyst}$ = 0.05 g, V_{water} = 110 mL.

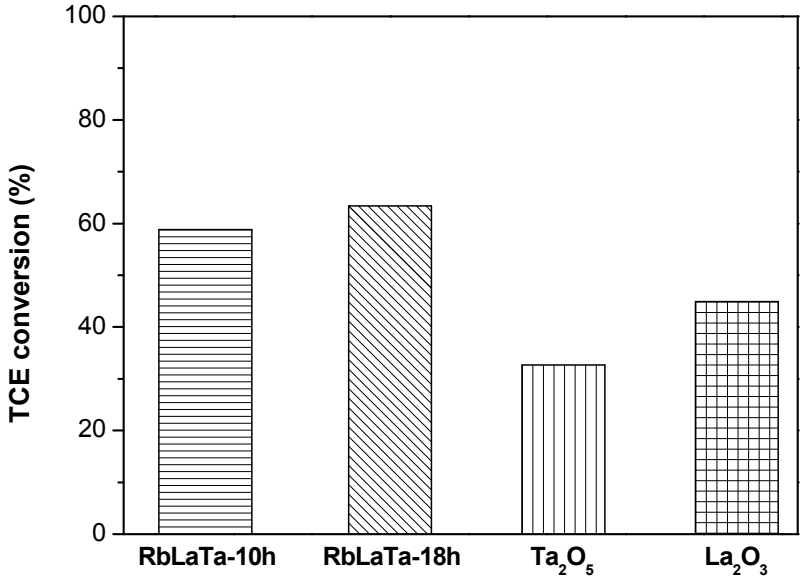

Fig. 7 – Conversion of TCE over the RbLaTa-10h and RbLaTa-18h photocatalysts and the reference compounds after 5 hours of simulated solar irradiation.

Fig. 8 shows the chlorine distribution (in mol. %) at the end of reaction, after 5 hours of simulated solar irradiation. The most efficient photomineralization catalyst, in terms of Cl^- formation, is RbLaTa-10h (≈ 29 mol. %) followed by RbLaTa-18h (≈ 20 mol. %), La_2O_3 (≈ 5 mol. %) and Ta_2O_5 (≈ 2 mol. %). Once again, the as-synthesized RbLaTa-based photocatalysts exhibited better photomineralization efficiency compared to the parental references.

The results depicted in Fig. 8 reveal that high surface area favors the conversion of TCE in intermediate chlorinated compounds (*i.e.* RbLaTa-18h) but, on the other hand, the sample with larger pool of surface -OH groups (RbLaTa-10h) is more active to mineralize TCE and clorinated intermediates to Cl^- and CO_2. Practically, the OH^- groups react with holes to form hydroxyl radicals (•OH), thus enhancing the photomineralization of TCE to Cl^-. Moreover, RbLaTa-10h presents a lower E_g value which also improves its activity. These are the reasons why RbLaTa-10h layered perovskite is a suitable catalyst for photomineralization of TCE compared to RbLaTa-18h solid.

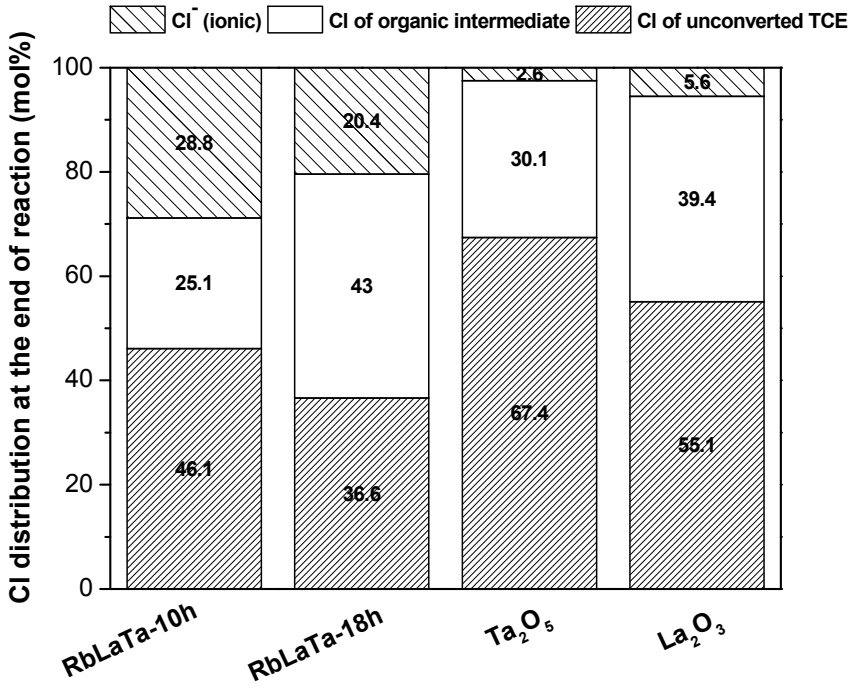

Fig. 8 – Distribution of chlorine at the end of reaction over the RbLaTa-10h (18h) catalysts and the reference compounds. The organic chlorine represents the sum of chlorine from organic intermediate and chlorine from unconverted TCE.

CONCLUSION

Two samples of $RbLaTa_2O_7$ layered perovskites were prepared by solid-state reaction at 1100 °C and two reaction times (*i.e.* 10 h and 18 h) and investigated as catalysts for photomineralization of trichloroethylene. XRD patterns confirm that $RbLaTa_2O_7$ layered perovskite was the dominant phase after increasing the reaction time up to 18 h. SEM analysis of the sample treated at 1100 °C for 10 h showed the formation of $RbLaTa_2O_7$ nanowires which tended to form bundles along with agglomerated nanoparticles. A longer reaction time determined a decrease of bundles and a tendency of the nanowires to split on. The photocatalytic test revealed that RbLaTa-10h was the proper photomineralization catalyst in terms of anionic chlorine formation (≈ 28 mol.%), while RbLaTa-18h was the most active one being able to convert 63 % of TCE. The RbLaTa-based photocatalysts exhibited better catalytic performance compared to the commercial references. It can be stated that both synthesized layered perovskites are useful photocatalytic materials for removal of harmful chlorinated pollutants.

Acknowledgements: This work was financially supported through Grant PCCDI 46/2018 MALASENT.

REFERENCES

1. B. Huang, C. Lei, C. Wei and G. Zeng, *Environm. Internat.,* **2014**, *71*, 118.
2. Y. Liu, Z. Wei, Z. Feng, M. Luo, P. Ying and C. Li, *J. Catal*., **2001**, *202*, 200.
3. T. Tanimura, A. Yoshida and S. Yamazaki, *Appl.Catal. B: Environm*., **2005**, *61*, 346.
4. Z. Guo-Min, C. Zhen-Xing, X. Min and Q. Xian-Qing, *J. Photochem. Photobiol. A: Chem*., **2003**, *161*, 51.
5. R. State, F. Papa, T. Tabakova, I. Atkinson, C. Negrila and I. Balint, *J. Catal*., **2017**, *346*, 101.
6. J. C. Joo, C. H. Ahn, D. G. Jang, Y. H. Yoon, J. K. Kim, L. Campos and H. Ahn, *J. Hazard. Mater*., **2013**, *263*, 569.
7. H. Kato and A. Kudo, *J. Phys. Chem*., B, **2001**, *105*, 4285.
8. C. Ogata, S. Ida and Y. Matsumoto, *IOP Conf. Series: Materials Science and Engineering*, **2009**, *1*, 012004, doi:10.1088/1757-8981/1/1/012004.
9. M. Machida, J. Yabunaka and T. Kijima, *Chem. Mater.*, **2000**, *12*, 812.
10. B. Bakiz, F. Guinneton, M. Arab, A. Benlhachemi, S. Villain, P. Satre, and J.-R. Gavarri, *Advan. Mater. Sci. Eng.*, **2010**, art. ID 360597, 6 pag., http://dx.doi.org/10.1155/2010/360597.
11. V. Dimitrov and T. Komatsu, *J. Solid State Chem.*, **2012**, *196*, 574.
12. B. Jancar, M. Valant and D. Suvorov, *Chem. Mater*., **2004**, *16*, 1075.
13. N. Preux, A. Rolle, C. Merlin, M. Benamira, M. Malys, C. Estournes, A. Rubbens and R.N. Vannier, *C. R. Chimie*, **2010**, *13*, 1351.
14. T. Bezrodna, T. Gavrilko, G. Puchkovska, V. Shimanovska, J. Baran and M. Marchewka, *J. Molec. Struct*., **2002**, *614*, 315.
15. D. Arney and P. A. Maggard, *ACS Catal*., **2012**, *2*, 1711.
16. J. Hu, J. Ma, L. Wang and H. Huang, *J. Alloy. Compd*., **2014**, *583*, 539.